Title	Sedimentation and remobilization of radiocesium in the coast area of Ibaraki, 70 km south of the Fukushima Dai-ichi Nuclear Power Plant
Author(s)	Shigeyoshi Otosaka, Takuya Kobayashi
Citation	Environmental Monitoring and Assessment, 185(7) ; p.5419-5433
Text Version	Author Accepted Manuscript
URL	http://jolissrch-inter.tokai-sc.jaea.go.jp/search/servlet/search?5036704
DOI	http://dx.doi.org/10.1007/s10661-012-2956-7
Right	The final publication is available at link.springer.com.

Sedimentation and remobilization of radiocesium in the coastal area of Ibaraki, 70 km south of the Fukushima Dai-ichi Nuclear Power Plant

Shigeyoshi Otosaka*, Takuya Kobayashi

Research Group for Environmental Science, Japan Atomic Energy Agency

*Corresponding author:
Phone: +81-29-282-5171
Facsimile: +81-29-282-6760
e-mail: otosaka.shigeyoshi@jaea.go.jp

Abstract

Sedimentation and remobilization processes of radiocesium were investigated from time-series observations at 9 stations in the coastal area of Ibaraki, 70–110 km south of the Fukushima Dai-ichi Nuclear Power Plant (1FNPP). Sediment samples were collected 4 times between June 2011 and January 2012, and concentrations of radiocesium as well as sediment properties such as grain size and elemental compositions were analyzed. Cumulative inventory of ^{137}Cs in sediment (0–10 cm) ranged between 4×10^{3} and 3×10^{4} Bq/m^{2} as of January 2011. This amount was generally higher at stations nearer 1FNPP and has remained at the same level since August 2011. From these results, it can be inferred that dissolved radiocesium advected southward from the region adjacent to the 1FNPP and was deposited to the sediment of the study area in the early stage after the accident. The incorporation of radiocesium into sediments was almost irreversible, and higher concentrations of ^{137}Cs were obtained from the finer-grained fraction of sediments. In the northern offshore stations, resuspension of the fine-grained sediments formed a high-turbidity layer 10–20 m above the seabed. These results indicate that radiocesium-enriched fine particles were transported from the coast to offshore regions through the bottom high-turbidity layer.

Keywords: Radiocesium; Fukushima-Daiichi nuclear power plant; seabed sediment; coastal area; redistribution

Introduction

The accident of TEPCO's Fukushima Dai-ichi Nuclear Power Plant (1FNPP) released a large amount of anthropogenic radionuclides into the environment, and is still affecting people who are living in the surrounding regions. MEXT (2011a) reported that significant concentrations of anthropogenic radionuclides, such as iodine-131, cesium-134 (^{134}Cs), cesium-137 (^{137}Cs), tellurium-129m, silver-110m, niobium-95, and antimony-125, were detected from seabed sediments off the eastern regions of the main island of Japan. Since most of the short-lived radionuclides decayed to a level below the detection limit, two isotopes of radiocesium; ^{134}Cs and ^{137}Cs, have been considered as the major radionuclides that should be monitored from a viewpoint of radiological dose assessment.

The dominant aquatic species of cesium in seawater is the uncomplexed Cs^+ ion and there is a low tendency to form complexes in the marine environment. As the concentration of stable Cs in seawater is about 2 nmol/L and is almost constant in the ocean (Spencer et al. 1970), Cs is regarded as a "soluble" element. An estimation that the amount of ^{137}Cs in seabed sediment of the Japan Sea, a marginal sea of the North Pacific, accounts for only 4% of the total ^{137}Cs (Ito et al. 2007) also supports evidence that most of ^{137}Cs is dissolved in seawater.

However, more than 50 Bq/kg of radiocesium were detected from the sediment surface (MEXT 2011b) as well as from marine biota (Buesseler et al. 2012) collected at over 100 km away from the 1FNPP, and these concentration levels are significantly higher than values before the accident (3–4 Bq/kg, mainly due to global fallout) (MEXT 2012a). In addition, although concentrations of radiocesium in seawater near the facility decreased exponentially with time

58 (Buesseler et al. 2011; Aoyama et al. 2012), sedimentary radiocesium have
59 remained at high concentration levels at least for one year after the accident
60 (MEXT 2011a; 2012b). These results clearly show that radiocesium remains in
61 the seabed for an extended period of time.

62 Three major processes are known to accumulate cesium into marine particles.
63 One is the selective adsorption of Cs^+ by clay minerals, especially by vermiculite
64 and illite minerals (Comans et al. 1991; Comans and Hockley 1992; Sakuma and
65 Kawamura 2011). This process is attributable to the large ionic radius,
66 uncomplexing nature and low hydration energy of Cs. The second is electronic
67 bonding at the frayed edge sites (FES), external basalt sites, or within the
68 interlayer which leads to inner sphere complexes (e.g., Poinssot et al. 1999).
69 Adsorption through inner-sphere complexation is nearly irreversible and can limit
70 the Cs mobility and bioavailability (USEPA 1999; Lujanienė et al. 2005). The
71 third is incorporation of Cs^+ into marine biota. Cesium is usually accumulated in
72 soft tissue such as muscle, and the biological turnover time is less than 100 days
73 (Yamada 1997; Kasamatsu 1999; Bustamante et al. 2006). A potential to
74 adsorb/incorporate radiocesium on/into sediments by the first two processes
75 would be elevated in coastal regions because these processes occur when
76 dissolved radiocesium comes into contact with clay minerals. Bioaccumulation
77 of radiocesium can also be stimulated in coastal regions where higher biological
78 production and larger input of terrestrial materials are significant. Otosaka et al.
79 (2006) actually reported that the inventory of ^{137}Cs in sediment is larger in the
80 coastal regions of Japan.

81 Several simulation models in the region around the coast of Fukushima
82 calculated that contaminated waters released from the 1FNPP had generally
83 flowed southward in March and April 2011 (e.g., Kawamura et al. 2011; Tsumune

et al. 2012). As a consequence, in April 2011, significant concentrations of radiocesium over the provisional regulation value of fisheries products (500 Bq/kg-wet for radiocesium at that time) were detected from fishes (Japanese sandlance: *Ammodytes personatus*) caught in the coast of Ibaraki Prefecture, adjacent to Fukushima Prefecture (Fig. 1)(JFA 2011). The MEXT (2011c) reported that several monitoring stations off Ibaraki had locally-elevated concentrations of sedimentary radiocesium. They also reported that the temporal variations of the concentration at those stations were larger than those in other regions. Detailed and continuous observations of sedimentary radiocesium in the coastal area of Ibaraki are thus important to understand factors controlling the accumulation and remobilization of sedimentary radiocesium released by the accident.

Methods

Field sampling

Field observations were carried out at 9 stations in the coastal area of Ibaraki, 70–110 km south of the 1FNPP (Table 1; Fig. 1). 5 km west of Sta. S1, there is an estuary of Kuji River that is a major river in this region. Four stations were set up in the shallow region (Stas. S1–S4: bottom depth <50 m) to observe effects by the river discharges and coastal currents. In addition, five offshore stations (Stas. S5–S9) were set to observe the subsequent processes.

Four cruises of R/V *Seikai* (Japan Atomic Energy Agency) were conducted in July 20, August 23, October 27 in 2011, and January 18 in 2012. Sediment samples were collected using a Smith-McIntire sampler and cut into two layers: upper (0–3 cm) and lower (3–10 cm) layers on board the ship. Vertical

distributions of turbidity and temperature in the overlying water column were also measured using a turbidity sensor (JFE-Advantech Co., ATU-6-CMP) and a temperature-depth sensor (JFE-Advantech Co., ATD-HR), respectively.

Radiochemical/chemical analysis

After being transferred to a laboratory on land, sediment samples were dried at 105°C, crushed, and the coarse fractions were removed using a 2-mm sieve (MEXT 2004). Sieved sediment samples were filled in a plastic container, and specific gamma-rays of ^{134}Cs (604 and 795 keV) and ^{137}Cs (661 keV) were measured using a coaxial Ge detector (1.8–2.4 keV/1.33 MeV of resolution and 32–105% of efficiency). The precision of ^{134}Cs and ^{137}Cs measurements was <2% at ±1sigma. For subset of samples of which large enough amounts were obtained, further sieving was made using a 75-μm sieve and ^{137}Cs in each fraction was measured using a well type Ge detector (ORTEC GWL-120230, 2.3 keV/1.33 MeV of resolution). Concentrations of radiocesium reported in the following subsections are represented as Bq/kg by dry weight. The concentrations of radiocesium were decay-corrected to the date and time of the sampling.

For all samples, water content and dry bulk density for estimation of cumulative ^{137}Cs levels were measured with a given volume of plastic tube. Relative uncertainties in ^{137}Cs levels due to propagation of errors for gamma-ray counting and dry bulk density estimation are low, i.e., about 5%.

Size distribution of sediment samples was measured using a laser diffraction particle size analyzer (Shimadzu SALD-2000J). A subset of samples obtained in August 2011 was decomposed using a mixed acid solution in a Teflon-sealed vessel (Otosaka et al. 2004), and concentrations of the major components, silicon

(Si), aluminum (Al), calcium (Ca), sodium (Na), potassium (K), magnesium (Mg), manganese (Mn) and iron (Fe) were measured by spectrophotometry or ICP-atomic emission spectrometry. The loss of ignition method was used to determine the organic matter content: the samples were heated in a muffle furnace at 500°C for 24 hours.

Values of enrichment factor (EF) were determined by elemental compositions of major lithogenic elements, Si, Al, K, Mg, Fe, and Mn to assess the contribution of riverine materials on seabed sediment.

$$EF = ([M]/[Al])_X : ([M]/[Al])_{S1}, \quad (1)$$

where $[M]_X$ is the concentration of the chemical element M in sediment at Station X; $[Al]_X$ is Al concentration in sediment at Sta X; $[M]_{S1}$ and $[Al]_{S1}$ are the concentrations of the element in question and of Al in sediment at Sta. S1. Station S1, the nearest station from the river mouth, was selected as a reference station. Because the station is near the river mouth, it was assumed that the suspended material and seabed sediment predominantly consist of riverine material. In addition, Al was selected as a reference element because it is regarded as a conservative terrestrial element.

Speciation/Suspension experiments

Samples obtained from Stas. S1 (June 20, 2011) and S5 (August 23, 2011) were used for analysis of surface-exchangeable Cs and organically-bound Cs. Sta. S1 was selected as the closest station from the river mouth, and Sta. S5 was selected as a typical offshore station. The Cs speciation experiments were

159 carried out using the method of Lujanienė et al. (2005) and Mortlock and Froelich
160 (1989) with some modifications. Exchangeable Cs was extracted by adding 100
161 mL of 1 M ammonium acetate to 10 g of powdered sample in a centrifuge tube,
162 and reacted for 6 hours at room temperature. The extraction liquid was removed
163 by centrifugation and filtration through a 0.2-μm membrane filter. A half of the
164 residue (c.a. 5 g) was dried and used for ^{137}Cs measurement by a well type gamma
165 detector. Another half of the residue was used for subsequent extraction of
166 organically-bound Cs. A 30 mL aliquot of 10% hydrogen peroxide was added to
167 the residue in a centrifuge tube and allowed to react for 6 hours at room
168 temperature. The residue was dried and ^{137}Cs was measured using a well type
169 gamma detector.
170 Concurrently with the speciation experiments, a suspension experiment was
171 carried out to measure the desorption rate of radiocesium from the sediment to the
172 overlying seawater. Briefly, powdered sediment sample was mixed with
173 “uncontaminated” seawater at the ratio of 1:10 in a centrifuge tube. The tube
174 was mildly mixed 5 min/day using a shaker, and the procedure was repeated over
175 a period of 30 days. After 1, 5, 10, 20 and 30 days, liquid and solid fractions
176 were separated by the same procedure of the above-mentioned experiment. The
177 residue was dried and used for ^{137}Cs measurement. The “uncontaminated”
178 seawater used in this experiment was collected at 2000 m depth in the offshore
179 area of Ibaraki (36° 30’N 142° 00’E). ^{137}Cs concentration in the seawater was
180 less than 5 mBq/L, and was negligible for the experiment. Both speciation and
181 suspension experiments were carried out in duplicate.
182

Results

Distributions of ^{137}Cs concentration in the upper layer (0–3 cm) of sediment are shown in Fig. 2. On June 20, 2011, ^{137}Cs concentration ranged between 50 and 1020 Bq/kg, and was highest at the northernmost station, S4 (Fig. 2a). In a station about 10 km northeast of the Kuji river mouth (Sta. S2), where sediments consisted of coarse sand and granule, concentration of sedimentary ^{137}Cs (50 Bq/kg) was significantly lower than the other stations. No offshore data were taken on June 20. On August 23 (Fig. 2b), no local elevation of ^{137}Cs was observed, and differences of ^{137}Cs concentration between the stations were smaller than those in June. In the northeastern offshore stations (S5 and S6), ^{137}Cs concentrations were higher than those in the corresponding shallower stations (Stas S3 and S4, respectively). On October 27, ^{137}Cs concentrations were lower than those in August at all stations except for Sta. S7 (Fig. 2c). The decrease in ^{137}Cs concentration was remarkable at the shallower stations. On January 18 (Fig. 2d), a significant concentration (729 Bq/kg) was seen at Sta. S4, yet the southern stations (Stas. S1, S2, S7 and S8) had lower ^{137}Cs concentrations compared with those in October.

Vertical changes in ^{137}Cs concentration in sediment (Fig. 3) showed different characteristics between the shallow and the offshore stations. In the shallow region (Stas. S1–S4), less vertical changes were observed. At Sta. S4, on the contrary, ^{137}Cs concentration was higher in the lower layer. Such a significant vertical transport of ^{137}Cs to the deeper sediment is attributable to characteristics of the shallow region, such as penetration of ^{137}Cs-contaminated seawater through large pore spaces of sediments formed of coarse particles and/or efficient vertical mixing of sediments through bioturbation (Yeager et al., 2004).

208 At Stas. S3 and S4, where sediments consisted of fine sand, ^{137}Cs
209 concentrations of the lower sediment remarkably decreased between June and
210 August, and then remained the level after August 2011. On the other hand,
211 coarser sediment in Sta. S2 did not show any temporal change in ^{137}Cs
212 concentration. Decreases in ^{137}Cs concentration of the sandy sediments are
213 probably due to sporadic events such as disturbances stimulated by rough sea
214 conditions. A disturbance of seabed sediment can resuspend fine particles to the
215 bottom water. Because of their slow sinking speed, fine particles are easily
216 transported in relation to seawater movements. Although it is difficult to specify
217 the "event" based on limited information, disturbance by sediment resuspension
218 and subsequent remobilization of fine-grained sediments between June and
219 August could be a potential process to decrease ^{137}Cs the concentration in sandy
220 sediments.
221 In the offshore regions (Stas. S5–S9), concentrations of sedimentary ^{137}Cs in
222 3–10 cm layer were lower than those in the upper layer (except for Sta. 8 in
223 August), and few temporal variations were observed. As shown in Table 1, most
224 offshore sediments consist of very fine sand (c.a. <100 μm) of low permeability.
225 Expected velocity of bottom currents, about 10 cm/sec, hardly causes vertical
226 mixing of the sediment. At the offshore region, it can be inferred that a
227 diffusional vertical transport of ^{137}Cs in sediment dominated the distributions.
228 In addition, across the study area, considerable population of macrobenthos,
229 such as the polychaete Maldanidae (*Maldanella sp.*) were observed in the
230 sediment. Thus, bioturbation would also be expected to be a significant process
231 controlling vertical transport of ^{137}Cs in sediments.
232

Discussion

Accumulation processes of radiocesium in sediment in the coastal area of Ibaraki

Levels of ^{137}Cs cumulative for the upper 10 cm sediments (Bq/m^2) are summarized in Table 2. No data are shown for several stations where the lower sediment layer was not collected. Estimated ^{137}Cs levels in sediment ranged between 2.6 kBq/m^2 (Sta S9 on August 23) and 96 kBq/m^2 (Sta S4 on June 20). The ^{137}Cs levels were the same as those of a cumulative deposition of ^{137}Cs on the ground observed at Hitachinaka City, about 10 km southwest of Sta. S1 (25 kBq/m^2: Hirose 2012). ^{137}Cs levels in sediment decreased considerably between June and August, and then remained at the same level until January 2012. This trend indicates that the initial deposition of ^{137}Cs to the sediment had almost ceased by August, and that the incorporation of ^{137}Cs into sediments was almost irreversible.

In contrast to the distribution of ^{137}Cs concentrations in the sediment surface layer (Fig. 2), higher ^{137}Cs levels were observed in shallow regions (Table 2). The higher levels would be attributable to an efficient vertical transport of ^{137}Cs in sandy sediment in that region.

MEXT (2012c) reported that ^{137}Cs concentrations in upper sediments (0–3 cm) on the coast of Fukushima Prefecture (20–200 m depth) were 94–536 Bq/kg in April 2011 and 33–316 Bq/kg in January 2012. These concentrations were generally higher than those on the coast of Ibaraki Prefecture (Fig. 2) except for some locally-elevated data. The distributional pattern that sedimentary ^{137}Cs concentrations decrease with a distance from the 1FNPP was consistent with the local distribution of sedimentary ^{137}Cs (Fig. 2). ^{137}Cs levels in Table 2 also showed a latitudinal gradient, and the pattern seems to decrease southward with

259 distance from the 1FNPP. Two processes accumulating radiocesium in the
260 northern stations are considered –adsorption of dissolved radiocesium onto seabed
261 sediments and lateral (southward) transport of radiocesium-bound suspended
262 particles.

263 A monitoring survey held 3 weeks after the accident at 20 km south of the
264 facility (40 km north of our study area) observed 7.2 Bq/L of ^{137}Cs in the surface
265 seawater (MEXT 2011d). Assuming that the surface water was transported
266 southward along the coast at current speed 5 cm/sec, the expected ^{137}Cs flux
267 flowing into our study area through a vertical box (10 km width × 100 m depth) is
268 3×10^{13} Bq/day. On the other hand, assuming that an averaged concentrations of
269 suspended particles is 0.2 mg-dry/L (see subsection 4.3) and concentration of
270 ^{137}Cs in the suspended particles as 1 kBq/kg-dry (maximum concentration of
271 sedimentary ^{137}Cs obtained from this study), a lateral flux of suspended ^{137}Cs
272 though the lattice is estimated to be 9×10^{8} Bq/day, less than 1 permil of the
273 dissolved flux.

274 Cesium is known as a “soluble” element in seawater, and the abundance of
275 sedimentary ^{137}Cs in a typical marginal sea is quite low (Ito et al. 2007).
276 However, adsorption of Cs^{+} onto particles, such as sediment, is enhanced by the
277 presence of clay minerals, and the transfer is relatively fast (Santschi et al., 1983;
278 Nyffeler et al. 1984; Lujanienė et al. 2005). After the fallout from the
279 Chernobyl accident, for example, Santschi et al. (1990) noted that about 25% of
280 the ^{137}Cs deposited onto the lake surface was found within one year in sediments
281 of lakes with 50-100 m depths. Even if only 1% of the dissolved ^{137}Cs that
282 flowed into our study area is removed from the water column, in consideration of
283 a lower potential accumulation of ^{137}Cs into sediment in marine systems, the
284 adsorption would produce sedimentary ^{137}Cs at 3×10^{11} Bq/day (1% × 3×10^{13}

285 Bq/day), and the rate would be more than 100 times higher than that of the direct
286 input of particulate ^{137}Cs (9×10^{8} Bq/day). Therefore, it can be inferred that the
287 predominant process to produce the observed initial distribution of sedimentary
288 ^{137}Cs in the study area is the southward flow of contaminated seawater followed
289 by "*in-situ*" adsorption/incorporation on/into the seabed sediments.
290 At stations adjacent to the river mouth (Stas. S1 and S8), locally-elevated
291 levels of ^{137}Cs were observed. Obviously, riverine input of particulate
292 radiocesium is also important for increasing their levels in neritic sediments.
293 The contribution of riverine materials on seabed sediment is assessed here by
294 using values of enrichment factors (EFs). Estimated EFs (Table 3) in the
295 estuarine stations (Stas. S2, S8, and S9) indicated higher values of Mg (1.8±0.4)
296 and Fe (1.8±0.2), than those at the other stations (1.1±0.1 for Mg and 1.2±0.1 for
297 Fe, respectively). A qualitative analysis using X-ray diffraction also indicated
298 that the estuarine sediments showed a signature of clay minerals (data are not
299 shown). Considering that both Mg and Fe compose octahedral layers of the
300 lithogenic mineral group of smectites or montmorillonites (e.g., Seibold and
301 Berger 1993), it is reasonable that the riverine clay minerals were accumulated in
302 the stations, a short distance away from the river mouth.
303 Enrichment factors were also obtained from finer (<75 μm) sediment in the
304 northern four stations (Stas. S3–S6). The EFs at Stas. S3, S4 and S6 showed
305 similar values to those of the bulk sediment, but significantly higher at Sta. S4
306 (Table 3). Although Sta. S4 is located at 34 km away from the river mouth, a
307 previous study suggested that fine riverine particles can be transported northward
308 over such a distance (Nasu 1964). Incorporation of Mg^{2+} and/or Fe^{2+} in clay
309 minerals produces a net negative charge on the surface. Considering that
310 riverine fine particles effectively adsorb hydrated Cs^{+} onto their surface, it is

311 consistent with the explanation that the higher ^{137}Cs concentrations were obtained
312 at Sta. S4.
313 Typical river discharge of the major river flowing into the study region (Kuji
314 River) is about 40 m^3/sec (MLIT 2012), and typical concentration of suspended
315 solid in the river water are 50 g/m^3 (Nagano et al. 2003). The maximum ^{137}Cs
316 concentration in the riverbed sediment after the 1FNPP accident is 2.4 kBq/kg-dry
317 (MOE 2011). Assuming that suspend particles in river water have the same level
318 of ^{137}Cs concentration in riverbed sediment, a riverine input of particulate ^{137}Cs is
319 calculated to be 4×10^8 Bq/day. In the Kuji River watershed, discharge of
320 suspended radiocesium would be quite limited considering that most ^{137}Cs
321 originating from the Chernobyl accident was accumulated in the riverbed
322 (Matsunaga et al. 1991). Therefore, the estimated flux of particulate ^{137}Cs
323 (4×10^8 Bq/day) might be an overestimated and is much smaller than the
324 above-mentioned processes controlling an initial distribution of ^{137}Cs in the
325 seabed. Nevertheless, as the input of radiocesium in seawater is decreasing,
326 riverine suspended load would become an alternative primary source of ^{137}Cs to
327 the coastal sediments.
328

329 **Speciation of sedimentary radiocesium**

330 A number of processes controlling redistribution of sedimentary radiocesium
331 originating from the 1FNPP accident, including: (i) desorption of sediment-bound
332 radiocesium, (ii) lateral transport of radiocesium-enriched sediment to offshore
333 regions, and (iii) vertical transport of radiocesium to deeper sediments. At least
334 since August 2011, no temporal changes in ^{137}Cs concentration have been
335 observed from sediment below 3 cm depth (Fig. 3), and consequently, the

336 temporal variability of ^{137}Cs levels in sediment are limited (Table 2). This
337 indicates that radiocesium in the upper layer sediment should be considered to
338 assess the further remobilization of sedimentary radiocesium. Accordingly, the
339 process (iii) is insignificant here.

340 It is known that radiocesium in marine biota is accumulated in soft tissue
341 such as muscle (e.g., Yamada 1997; Bustamante et al. 2006), and the biological
342 half-lives (19–84 days) are relatively shorter than the physical one (30 years)
343 (Kasamatsu 1999). This indicates that dissolution of radiocesium-bound
344 biogenic components can easily decrease levels of sedimentary radiocesium. In
345 addition, exchanging surface-adsorbed radiocesium ions with the other univalent
346 ions (e.g., alkaline metals) would decrease radiocesium concentration in sediment.
347 Speciation of radiocesium in sediment is thus crucial to estimate the fate and
348 bioavailability of sedimentary radiocesium.

349 In Fig. 4, results of sequential extraction of surface-adsorbed and
350 organic-bound ^{137}Cs are shown. Organic matter content used in this experiment
351 was 4% at Sta. S1 and 6% at Sta. S5. For both sediment samples, contribution of
352 surface-adsorbed ^{137}Cs was less than 5% of the total ^{137}Cs, and organically-bound
353 ^{137}Cs was about 20%. This result indicated that organic matter can be a major
354 reservoir of the labile ^{137}Cs in seabed sediments. In order to reproduce *in-situ*
355 dissolution of organically-bound radiocesium, sediment samples were suspended
356 in uncontaminated seawater, and the dissolution process was monitored (Fig. 5).
357 As a result, more than 85% of ^{137}Cs remained in the sediment during 30 days of
358 the experiment, and the remaining fraction was almost constant.

359 In conclusion, more than 75% of ^{137}Cs in coastal sediments was incorporated
360 into “residual” fractions (i.e. lithogenic materials), and the
361 dissolution/decomposition of labile fractions was insufficient at reducing levels of

^{137}Cs in the sediment. In addition, it can also be inferred that the remarkable decrease in ^{137}Cs level between June and August 2011 (Table 3) was not caused by dissolution of labile ^{137}Cs but by a physical transport (export) of irreversibly bound ^{137}Cs.

Remobilization of radiocesium-bound sediment from coast to the deep ocean

Relationship between particle size and ^{137}Cs concentration in sediment (upper layer) is shown in Fig. 6. For all sampling dates, ^{137}Cs concentrations decreased with increasing particle size. The ^{137}Cs–size relationship was almost stable after August 2011, and it seems that ^{137}Cs was selectively enriched in silt particles (c.a. <100 μm). Many researchers have pointed out the selective adsorption of radiocesium onto the fine-grained sediments predominantly due to their larger specific surface area and higher content of clay minerals (e.g., Fukui 1988; Abril and Fraga 1996). A series of surveys on the Japanese coastal areas during the 1960s found that ^{137}Cs derived from global fallout was selectively accumulated in muddy sediments rather than sandy ones (Nagaya and Saiki 1967). Silty sediments have a high mobility on the sediment-water boundary (e.g., Hjulstrøm 1935). Considering that silty sediments are broadly distributed along the 100 m isobaths along the coast of Fukushima and Ibaraki Prefectures (Nasu 1964; Aoyagi and Igarashi 1999), the silt particles would be a potential carrier of radiocesium to deposit radiocesium to offshore areas.

Although a significant temporal change in the ^{137}Cs–size relationship (Fig. 6) was seen between June and August, 2011, it hardly explains the process that coarse sediments with more than 100 μm were transported directly to offshore areas in the 2 months. Considering that the smaller fraction of sediment (<75

388 μm) had 1.5–6 times higher ^{137}Cs content compared with the coarser fraction
389 (Table 4), it can be inferred that ^{137}Cs-enriched fine sediments were selectively
390 exported from the surface sediment in the early stage after the accident, and
391 consequentially reduced the ^{137}Cs concentrations in the sediment surface.
392 In order to address resuspension and subsequent transport of fine-grained
393 sediments, distributions of turbidity, an indicator of the concentration of the
394 suspended particulate matter (SPM), in the water column were observed at the
395 offshore stations (Stas. S5–S9) in August 2011 and January 2012. At the
396 northern stations S5, S6 and S7, where the higher concentrations of ^{137}Cs were
397 seen in the sediment, high turbidities were observed 20–30 m above the bottom
398 (Fig. 7). Similar distributional patterns were observed in August 2011 and
399 January 2012. The high turbidity is considered to represent suspension of
400 radiocesium-bound fine sediments, and the bottom layer can be regarded as the
401 lateral “passage” of particulate radiocesium. Another survey above the shelf
402 break (about 20–30 km east of the sampling area of this study) also observed high
403 turbidities on the seafloor, and the highest turbidity corresponded to about 1
404 mg-dry/L of SPM concentration. In addition, the high turbidity layer on the
405 shelf break was propagated to 50–100 m of thickness. Seawater of the high
406 turbidity layer had higher density (mainly due to the lower temperature) and the
407 property was almost homogenous in the bottom layer. In the coast of Fukushima
408 and Ibaraki Prefectures, several water masses such as the Kuroshio (primary warm
409 current), Oyashio (primary cold current), and Tsugaru Warm Current waters are
410 coexisting in a complex fashion (e.g., Hanawa and Mitsudera 1987), and a front
411 formed by a dynamic balance between adjacent water masses reaches to the
412 seabed (Kubo 1988). High turbidities observed in the bottom water off Ibaraki

(Fig. 7) were probably developed by a formation of the benthic front and subsequent resuspension of fine-grained sediments.

As the bottom water dynamics become weaker in the offshore region, a potential carrier redistributing radiocesium would become finer. Because the contribution of the finer fraction is quite small, an extensive remobilization of sedimentary radiocesium would not be expected. This prediction can also be applied to the shallow regions. As shown in Table 4, as of August 2011, more than 70% of sedimentary ^{137}Cs is contained in the coarse fraction (>75 μm). Even though the finer fraction has a higher ^{137}Cs content, coarse sediments with lower mobility are the major reservoir of radiocesium in the region. This result indicates that ^{137}Cs initially deposited on the seafloor would not show an extensive export from the shallow region, unless exceptionally strong storms resuspend the seabed sediments.

Nevertheless, as mentioned above, in estuaries and the surrounding regions, riverine supply of SPM would keep accumulating radiocesium to the seabed. In these regions, riverine input and the subsequent redistribution of radiocesium through the bottom “passage” should be monitored over the long term.

Conclusion

From distributions of sedimentary radiocesium and oceanographic characteristics observed in the coastal area of Ibaraki, the following transport processes of sedimentary radiocesium can be inferred.

1) Major distributional patterns of the 1FNPP-derived radiocesium in coastal sediments were established within half a year after the accident.

2) Higher levels of sedimentary radiocesium in the shallow regions are attributable to a higher contact probability of dissolved radiocesium with sediment as well as the efficient vertical transport of radiocesium to the deeper layer of sediment via bioturbation.

3) Most of radiocesium in the coastal sediments is incorporated into lithogenic fractions, and this incorporation is almost irreversible. Accordingly, the biological availability of sedimentary radiocesium is relatively low, but continuous monitoring of radiocesium in marine biota is highly recommended because significant amounts of radiocesium have been accumulated in the sediment.

4) Radiocesium is selectively accumulated in finer-grained sediments. Resuspension and lateral transport of the fine-grained sediments plays an important role to redistribute the sedimentary radiocesium. Locally-elevated concentrations of radiocesium in surface sediment would indicate a “snapshot” of the subsequent transport of radiocesium-enriched fine sediments.

5) In the study area, as of January 2012, riverine inputs of suspended particulate matter can be regarded as a minor process to accumulate radiocesium in the coastal sediments. Nevertheless, its relative contribution would be expected to increase later years.

Acknowledgements

Field and analytical supports were provided by staff members of Radiation Protection Dept., Nuclear Fuel Cycle Engineering Lab., JAEA. This investigation benefited enormously and was vastly improved through discussions with Drs. M. Chino, A. Endo, H. Nagai, T. Matsunaga, H. Kawamura, T. Suzuki (JAEA), S. Igarashi (Fukushima Pref.), Y. Kato, and H. Narita (Tokai Univ.). We are also grateful to two anonymous reviewers for their constructive comments on the paper.

References

Abril, J.M, & Fraga, E. (1996). Some physical and chemical features of the variability of Kd distribution coefficients for radionuclides. Journal of Environmental Radioactivity, 30, 253-270.

Aoyagi, K., & Igarashi, C. (1999). On the size distribution of sediments in the coastal sea of Fukushima Prefecture. Bulletin of the Fukushima Prefectural Fisheries Experimental Station, 8, 69-81 (in Japanese).

Aoyama, M., Tsumune, D., & Hamajima, Y. (2012). Distribution of ^{137}Cs and ^{134}Cs in the North Pacific Ocean: impacts of the TEPCO Fukushima-Daiichi NPP accident. Journal of Radioanalitical Nuclear Chemistry, DOI: 10.1007/s10967-012-2033-2.

Buesseler, K.O., Aoyama, M, & Fukasawa, M. (2011). Impacts of the Fukushima Nuclear Power Plants on marine radioactivity. Environmental Science and Technology, 45, 9931-9935.

Buesseler, K.O., Jayne, S.R., Fisher, N.S., Rypina I.I., Baumann, H., Baumann, Z., Breier, C.F., Douglass, E.M., George, J., Macdonald, A.M., Miyamoto, H., Nishikawa, J., Pike, S.M., & Yoshida, S. (2012). Fukushima-derived radionuclides in the ocean and biota off Japan. Proceedings of the National Academy of Science, 109, 5984-5988.

Bustamante, P., Teyssie, J.L., Fowler, S.W., & Warnau, M. (2006). Assessment of the exposure pathway in the uptake and distribution of americium and cesium in cuttlefish (*Sepia officinalis*) at different stages of its life cycle. Journal of Experimental Marine Biology and Ecology, 331, 198-207.

Comans, R.N.J., Haller, M., & DePreter, P. (1991). Sorption of cesium on illite: Non-equilibrium behavior and reversibility. Geochimica et Cosmochimica Acta, 55, 433-440.

Comans, R.N.J., & Hockley, D. (1992). Kinetics of cesium sorption on illite. Geochimica et Cosmochimica Acta, 56, 1157-1164.

Fukui, M. (1988). Uptake of radionuclides onto suspended particulate matter in coastal water. J Nuclear Science and Technology, 25, 934-942.

Hanawa, K., & Mitsudera, H. (1987). Variation of water system distribution in the Sanriku coastal area. Journal of the Oceanographic Society of Japan, 42, 435-446.

Hjulstrøm, F. (1935). Studies of the morphological activity of rivers as illustrated by the River Fyris. Bulletin of the Geological Institution of the University of Upsala, 25, 221-527.

Hirose, K. (2012). Fukushima Dai-ichi nuclear power plant accident: summary of regional radioactive deposition monitoring results. Journal of Environmental Radioactivity, 111, 13-17.

Ito, T., Otosaka, S., Kawamura, H. (2007). Estimation of total amounts of anthropogenic radionuclides in the Japan Sea. Journal of Nuclear Science and Technology, 44, 912-922.

JFA (Japan Fisheries Agency) (2011). http://www.jfa.maff.go.jp/e/inspection/pdf/201103-09_kekka_en.pdf. Accessed on May 16, 2012.

Kasamatsu, F. (1999). Marine organisms and radionuclides –With special reference to the factors affecting concentration of ^{137}Cs in marine fish–. Radioisotopes, 48, 266-282 (In Japanese).

Kawamura, H., Kobayashi, T., Furuno, A., In, T., Ishikawa, Y., Nakayama, T., Shima, S., & Awaji, T. (2011). Preliminary numerical experiments on oceanic dispersion of ^{131}I and ^{137}Cs discharged into the ocean because of the Fukushima Daiichi Nuclear Power Plant Disaster. Journal of Nuclear Science and Technology, 48, 1349-1356.

Kubo, H. (1988). Research on the oceanographic conditions of Kashima-Nada, off the east coast of Honshu. Bulletin of the Ibaraki Prefectural Fisheries Experimental Station, 26, 1-98 (in Japanese with English summary and captions).

Lujanienė, G., Vilimaitė-Šilobritienė, B., Jokšas, K. (2005). Accumulation of ^{137}Cs in bottom sediments of the Curonian Lagoon. Nucleonika, 50, 23-29.

Matsunaga, T., Amano, H., & Yanase, N. (1991). Discharge of dissolved and particulate ^{137}Cs in the Kuji River, Japan. Applied Geochemistry, 6, 159-167.

MEXT (Ministry of Education, Culture, Sports, Science and Technology) (2004). Gamma-ray spectrometry using a germanium detector. Radioactivity Measurement Series No. 7. Tokyo: Ministry of Education, Culture, Sports, Science and Technology (In Japanese).

MEXT (2011a). http://radioactivity.mext.go.jp/en/contents/4000/3325/24/1305745_0527.pdf. Accessed on July 2, 2012.

MEXT (2011b). http://radioactivity.mext.go.jp/en/contents/4000/3324/24/1305745_0612.pdf. Accessed on July 2, 2012.

MEXT (2011c). http://radioactivity.mext.go.jp/en/contents/4000/3331/24/1350_1108.pdf. Accessed on July 2, 2012.

MEXT (2011d). http://radioactivity.mext.go.jp/en/contents/4000/3312/24/1304193_0331.pdf. Accessed on July 2, 2012.

MEXT (2012a) Database of Environmental Radioactivity. http://search.kankyo-hoshano.go.jp. Accessed on July 2, 2012 (in Japanese).

MEXT (2012b) http://radioactivity.mext.go.jp/en/contents/4000/3334/24/1350_012514.pdf. Accessed on July 2, 2012.

MEXT (2012c) http://radioactivity.mext.go.jp/en/contents/4000/3285/24/1330_030114.pdf. Accessed on July 2, 2012.

MLIT (Ministry of Land, Infrastructure and Transport, Japan) (2012). River Discharges Year Book of Japan, Year 2007. Tokyo: Japan River Association.

MOE (Ministry of Environment, Japan) (2011). http://www.env.go.jp/jishin/monitoring/result_pw111202.pdf. Accessed on July 2, 2012.

Mortlock, R.A., & Froelich, P.N. (1989). A simple method for the rapid determination of biogenic opal in pelagic marine sediments. Deep-Sea Research, 36, 1415-1426.

Nagano, T., Yanase, N., Tsuduki, K., & Nagao, S. (2003). Particulate and dissolved elemental loads in the Kuji River related to discharge rate. Environment International, 28, 649-658.

Nagaya, Y., & Saiki, M. (1967). Accumulation of radionuclides in coastal sediment of Japan (I) Fallout radionuclides in some coastal sediments in 1964-1965. Journal of Radiation Research, 8, 37-43.

Nasu, N. (1964). The provenance of the coarse sediments on the continental shelves and the trench slopes off the Japanese Pacific coast. In R.L. Miller (Ed.), Papers in Marine Geology (pp. 65-101). New York: Macmillan Co.

Nyffeler, U.P., Li, Y.H., & Santschi, P.H. (1984). A kinetic approach to describe trace-element distribution between particles and solution in natural aquatic systems. Geochimica et Cosmochimica Acta, 48, 1513-1522.

Otosaka, S., Togawa, O., Baba, M., Karasev, E., Volkov, Y.N., Omata, N., & Noriki, S. (2004). Lithogenic flux in the Japan Sea measured with sediment traps. Marine Chemistry, 91, 143-163.

Otosaka, S., Amano, H., Ito, T., Kawamura, H., Kobayashi, T., Suzuki, T., Togawa, O., Chaykovskaya, E.L., Lishavskaya, T.S., Novichkov, V.P., Karasev, E.V., Tkalin, A.V., & Volkov, Y.N. (2006). Anthropogenic radionuclides in sediment in the Japan Sea: distribution and transport processes of particulate radionuclides. Journal of Environmental Radioactivity, 91, 128-145.

Poinssot, C., Baeyens, B., & Bradbury, M.H. (1999). Experimental and modeling studies of caesium sorption on illite. Geochimica et Cosmochimica Acta, 63, 3217-3227.

Seibold, E., & Berger, W.H. (1993). Deep-Sea sediments –patterns, processes, and stratigraphic methods. In E. Seibold, & W.H. Berger (Eds.), The Sea Floor (pp. 215-240). Berlin: Springer.

Santschi, P.H., Bower, P., Nyffeler, U.P., Azevedo, A., & Broecker, W.S. (1983). Estimates of the resistance to chemical transport posed by the deep-sea boundary layer. Limnology and Oceanography, 28, 899-912.

Santschi, P.H., Bollhalder, S. Zingg, S., Lueck, A., & Farrenkothen, K. (1990). The self-cleaning capacity of surface waters after radioactive fallout. Evidence from European waters after Chernobyl, 1986-1988. Environmental Science and Technology, 24, 519-527.

Sakuma, H., & Kawamura, K. (2011). Structure and dynamics of water on Li^+-, Na^+-, K^+-, Cs^+-, H_3O^+-exchanged muscovite surfaces: A molecular dynamics study. Geochimica et Cosmochimica Acta, 75, 63-81.

Spencer, D.W., Robertson, D.E., Turekian, K.K., & Folsom, T.R. (1970). Trace element calibrations and profiles at the GEOSECS test station in the northeast Pacific Ocean. Journal of Geophysical Research, 75, 7688-7696.

Tsumune, D., Tsubono, T., Aoyama, M., & Hirose, K. (2012). Distribution of oceanic ^{137}Cs from the Fukushima Dai-ichi Nuclear Power Plant simulated numerically by a regional ocean model. Journal of Environmental Radioactivity, 111, 100-108.

USEPA (United States Environmental Protection Agency)(1999). Understanding variation in partition coefficient, Kd, values Vol. II: Review of geochemistry and available Kd values for cadmium, cesium, chromium, lead, plutonium, radon, strontium, thorium, tritium (^3H), and uranium. EPA 402-R-99-004B. Washington, DC: Office of Air and Radiation, U.S. Environmental Protection Agency.

585 Yamada, M. (1997). $^{239+240}$Pu and ^{137}Cs concentrations in salmon (*Oncorhynchus keta*) collected
586 on the Pacific coast of Japan. Journal of Radioanalytical Nuclear Chemistry, 223,
587 145-148.
588 Yeager, K.M., Santschi, P.H., & Rowe, G.T. (2004). Sediment accumulation and radionuclide
589 inventories (^{239,240}Pu, ^{210}Pb and ^{234}Th) in the northern Gulf of Mexico, as influenced by
590 organic matter and macrofaunal density. Marine Chemistry, 91, 1-14.
591

592 Figure captions

593 Figure 1 Sampling stations

594 Figure 2 Distributions of ^{137}Cs concentration in sediment surface (0–3 cm) layer; (a) June 2011,
595 (b) August 2011, (c) October 2011, and (d) January 2012.

596 Figure 3 Vertical distributions of ^{137}Cs concentration in sediment. Note the difference in
597 horizontal scale for S4 for June 20, 2011 and for Jan 18, 2012. Dashed line at 500 Bq/kg indicates
598 the range shown for the other stations.

599 Figure 4 Speciation of ^{137}Cs in sediment (0–3 cm layer) obtained from Stas. S1 (on June 20,
600 2011) and S5 (on August 23, 2011). See text for the detail.

601 Figure 5 Changes in remaining fraction of ^{137}Cs in sediment as a function of elapsed time (days)
602 after starting the suspension experiment.

603 Figure 6 Relationship between ^{137}Cs concentration in sediment (0–3 cm layer) and particle size.

604 Figure 7 Vertical distributions of turbidity observed at five offshore stations in August 2011 (left
605 panels) and January 2012 (right panels). With regard to unit of X-axis, 1 FTU (Formazin
606 Turbidity Unit) of turbidity approximately corresponds to 1 mg-dry/L of SPM concentration.
607

608 Table 1

609 Locations of sampling station and size class of sediments

Station	North latitude		East longitude		Depth	Wentworth size class
	Deg	Min	Deg	Min	m	
S1	36	30.1	140	40.6	30	Sand
S2	36	35.4	140	44.0	35	Coarse silt - Granule
S3	36	40.8	140	47.3	47	Fine sand / Medium sand
S4	36	46.1	140	47.3	26	Very fine sand / Fine sand
S5	36	46.1	140	53.9	75	Very fine sand
S6	36	40.8	140	53.9	95	Very fine sand
S7	36	35.4	140	50.6	90	Very fine sand
S8	36	30.1	140	47.3	75	Very fine sand / Fine sand
S9	36	24.8	140	47.3	86	Medium sand

610

611

612 Table 2

613 ^{137}Cs inventory in sediment cumulative to 10 cm depth

Station	^{137}Cs inventory (kBq/m^2)			
	20-Jun-11	23-Aug-11	27-Oct-11	18-Jan-11
S1	44.3±1.6	No data	No data	No data
S2	7.7±0.4	No data	11.9±0.5	No data
S3	34.6±1.4	18.8±0.7	13.1±0.5	11.0±0.4
S4	96.3±3.5	24.1±1.0	18.8±0.8	27.4±1.0
S5	No data	14.9±0.5	10.0±0.4	12.2±0.4
S6	No data	15.0±0.5	5.5±0.2	5.2±0.2
S7	No data	3.5±0.1	6.5±0.3	4.5±0.2
S8	No data	11.1±0.4	15.2±0.6	3.7±0.1
S9	No data	2.6±0.1	No data	No data

614

615

Table 3

Enrichment factors (EFs) of major components in bulk and size-fractioned (<75 μm) sediments. All samples were collected on August 23, 2011 and the upper layer was used for analysis. See text for the calculation of EFs.

Station	Si	K	Mg	Fe	Mn
S1	1.00	1.00	1.00	1.00	1.00
S2	1.11	0.99	**1.73**	**1.63**	1.98
S3	1.05	0.92	1.20	1.30	0.90
S4	0.95	0.88	1.30	1.24	1.50
S5	0.97	0.91	0.94	1.02	0.81
S6	0.94	0.94	1.26	1.25	0.91
S7	1.14	0.91	1.14	1.22	0.86
S8	1.02	0.77	**1.62**	**1.63**	1.11
S9	1.35	0.95	**2.33**	**1.94**	1.99
S3 (<75 μm)	1.01	0.84	1.12	1.16	1.17
S4 (<75 μm)	1.05	0.76	**1.91**	**1.85**	2.76
S5 (<75 μm)	1.11	0.86	0.86	0.91	0.84
S6 (<75 μm)	1.10	0.84	0.97	1.02	0.86

Table 4

^{137}Cs concentrations in size-fractioned sediments. All samples were collected on August 23, 2011.

Station	Layer	Grain size	^{137}Cs	F_p^*	F_{Cs}^{**}
	cm	μm	Bq/kg	%	%
S3	0-3	<75	257±6	15	24
		>75	148±4	85	76
S4	0-3	<75	819±7	5	24
		>75	135±3	95	76
S5	0-3	<75	379±5	42	51
		>75	255±5	59	49
S6	0-3	<75	329±6	54	48
		>75	428±7	46	52

*Composition ratio of each fraction to bulk sediment

**Composition ratio of ^{137}Cs in each fraction to total ^{137}Cs

631 Appendix A1

632 Bulk densities, ^{134}Cs and ^{137}Cs concentrations, and grain size of sediment samples.

Date	Station	Sampling time (JST)	Layer	DBD*	^{134}Cs	^{137}Cs	Grain size
			cm	g/mL	Bq/kg-dry	Bq/kg-dry	Phi
2011/6/20	S1	10:00	0-3	1.36	388±1	420±1	1.5
			0-3	1.29	278±5	300±4	No data
	S2	10:45	0-3	1.97	45±2	50±2	<-1
			3-10	1.99	29±2	34±1	<-1
	S3	11:20	0-3	1.36	216±1	236±1	1.8
			3-10	1.34	242±5	266±4	2.7
	S4	11:54	0-3	1.19	955±2	1020±1	2.9
			3-10	1.20	647±7	716±6	
2011/8/23	S1	10:12	0-3	0.73	131±1	139±1	3.3
	S2	10:55	0-3	0.69	173±1	190±1	4.3
	S3	11:26	0-3	1.11	148±1	169±1	2.4
			3-10	1.18	137±1	159±1	2.7
	S4	12:04	0-3	1.16	155±1	168±1	2.9
			3-10	1.30	176±1	201±0	2.9
	S5	12:41	0-3	0.76	304±1	346±1	3.5
			3-10	0.94	91±1	107±1	3.7
	S6	13:21	0-3	0.57	377±3	397±2	3.9
			3-10	0.71	143±1	166±1	3.8
	S7	14:15	0-3	0.85	78±0	89±0	3.4
			3-10	1.16	13±0	16±0	2.9
	S8	14:55	0-3	0.93	127±1	144±1	2.2
			3-10	1.13	76±0	90±0	3.9
	S9	14:50	0-3	1.15	34±0	38±0	1.3
			3-10	1.26	12±0	14±0	1.5
2011/10/27	S1	10:08	0-3	1.00	57±1	69±1	3.3
	S2	10:43	0-3	1.62	47±1	55±1	0.7
			3-10	1.72	64±1	77±1	<0.5
	S3	11:18	0-3	1.28	78±1	97±1	2.2
			3-10	1.29	86±1	104±1	2.2
	S4	11:52	0-3	1.31	60±0	73±1	2.9
			3-10	1.23	151±1	185±1	2.8
	S5	12:23	0-3	0.75	187±2	211±1	3.7
			3-10	0.96	67±0	79±0	3.6
	S6	12:53	0-3	0.85	122±1	140±1	3.5
			3-10	0.93	24±0	30±0	3.6

	S7	13:36	0-3	0.79	174±2	195±1	3.7
			3-10	1.11	19±0	24±0	3.6
	S8	14:12	0-3	0.99	99±1	113±1	3.2
			3-10	1.33	107±1	127±1	2.7
2012/1/18	S1	10:10	0-3	1.17	35±0	46±0	<0.5
	S2	10:50	0-3	1.08	51±0	67±0	5.5
	S3	11:35	0-3	1.30	81±0	105±0	2.9
			3-10	1.30	58±0	76±0	2.1
	S4	12:00	0-3	0.48	557±1	729±1	3.6
			3-10	0.98	188±1	247±1	No data
	S5	12:35	0-3	0.69	212±1	281±1	3.5
			3-10	0.79	92±1	115±1	3.5
	S6	13:14	0-3	0.76	117±1	156±1	3.4
			3-10	0.89	19±0	26±0	3.7
	S7	14:02	0-3	0.86	71±0	91±0	3.4
			3-10	1.08	21±0	28±0	4.0
	S8	14:47	0-3	1.04	41±0	54±0	2.8
			3-10	1.09	19±0	26±0	2.3

633 *DBD: Dry bulk density

634 Activities of ^{134}Cs and ^{137}Cs were decay-corrected to sampling date.

635 Uncertainties are given 1-sigma counting errors.

636 Appendix A2

637 Concentrations of major components in sediment. All samples were collected on August 23,
638 2011.

Station	Concentration (%)							
	Si	LOI*	Al	Fe	Ca	K	Mg	Mn
S1	28.0	4.53	6.85	2.68	1.83	1.71	1.00	0.05
S2	27.6	5.55	6.07	3.87	2.00	1.51	1.53	0.09
S3	27.3	3.59	6.37	3.25	2.06	1.47	1.11	0.04
S4	25.6	3.30	6.55	3.18	2.44	1.45	1.24	0.08
S5	26.8	6.42	6.74	2.68	1.27	1.54	0.92	0.04
S6	25.3	6.57	6.55	3.21	1.21	1.54	1.20	0.05
S7	30.7	6.53	6.57	3.14	1.52	1.49	1.09	0.04
S8	26.7	3.40	6.38	4.08	2.96	1.24	1.50	0.06
S9	32.1	2.00	5.81	4.41	1.67	1.38	1.97	0.09
S3 (<75 um)	28.1	5.34	6.78	3.07	1.68	1.42	1.11	0.06
S4 (<75 um)	27.4	3.18	6.39	4.63	2.56	1.21	1.78	0.14
S5 (<75 um)	32.5	4.36	7.13	2.55	1.34	1.53	0.90	0.05
S6 (<75 um)	31.6	6.39	7.04	2.81	1.39	1.48	1.00	0.05

639 *Loss of ignition

640

641

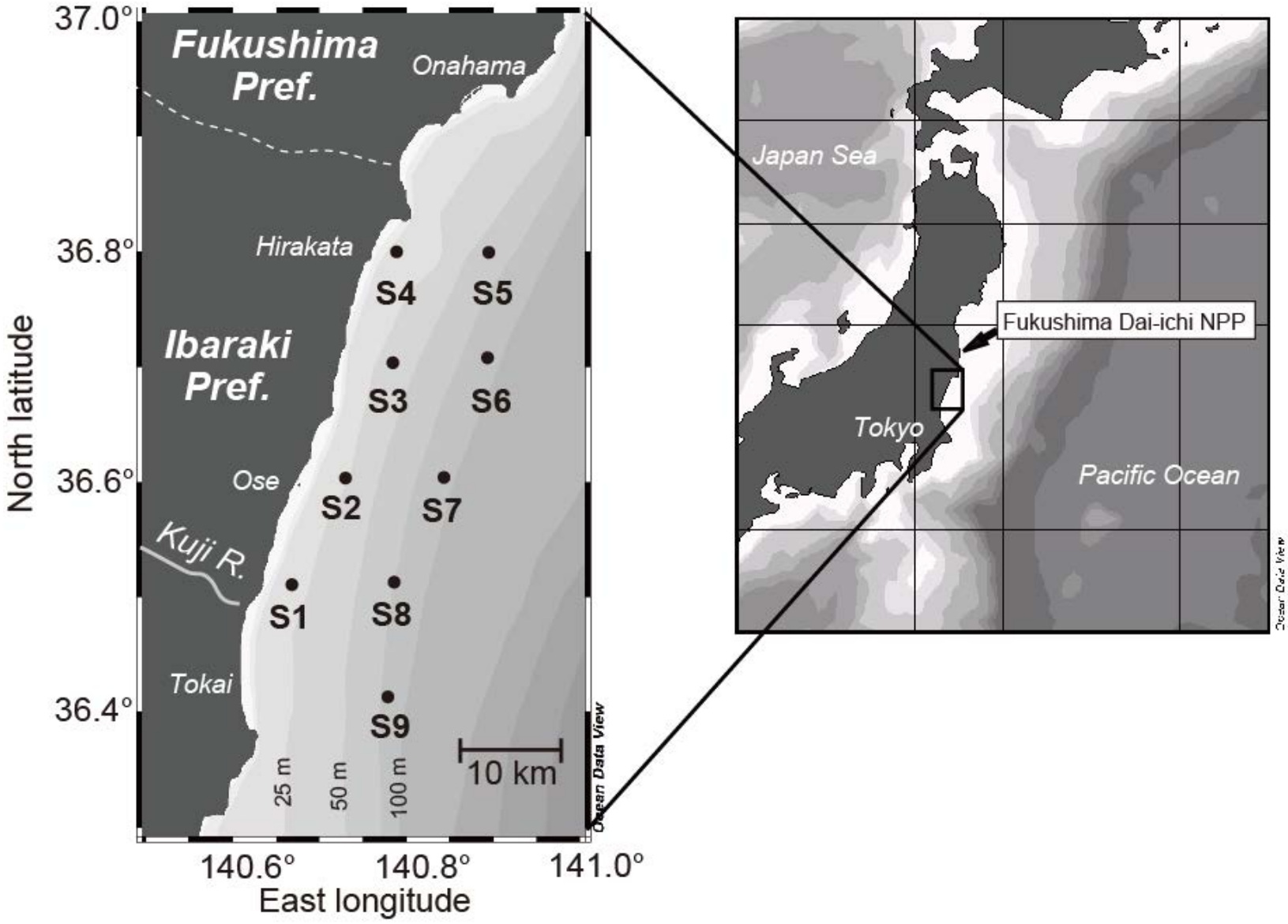

Otosaka and Kobayashi, Fig 1

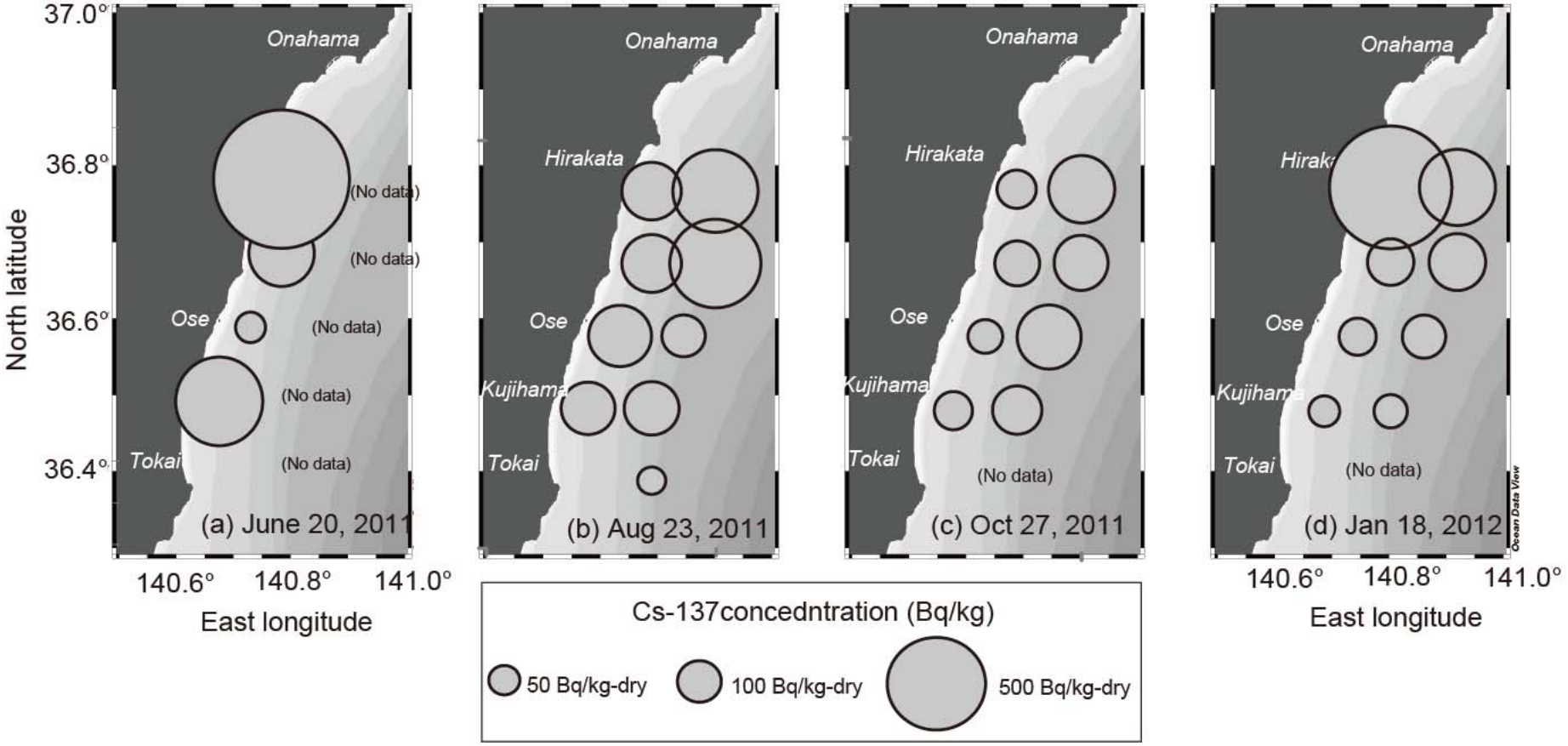

Otosaka and Kobayashi, Fig 2

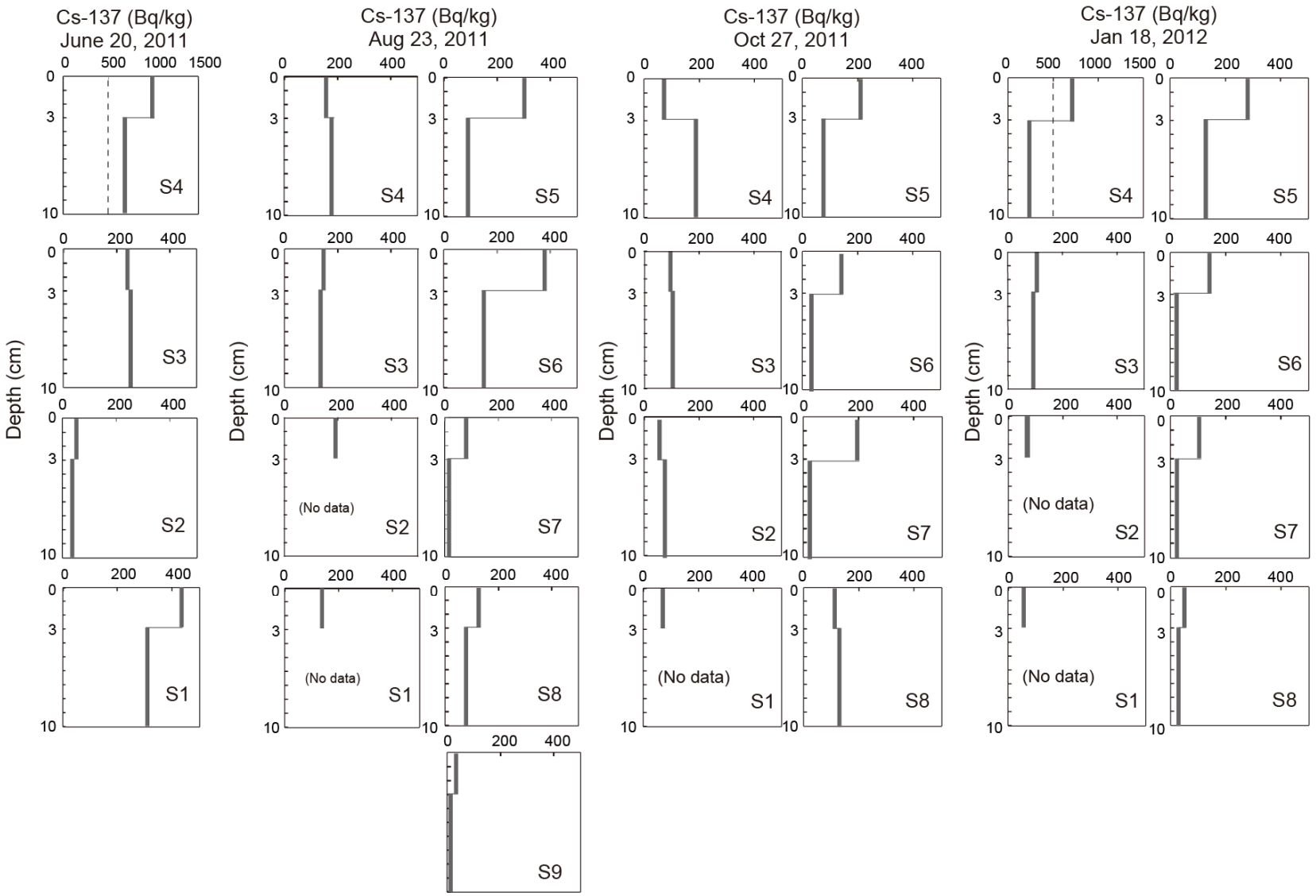

Otosaka and Kobayashi, Fig 3

Otosaka and Kobayashi, Fig 4

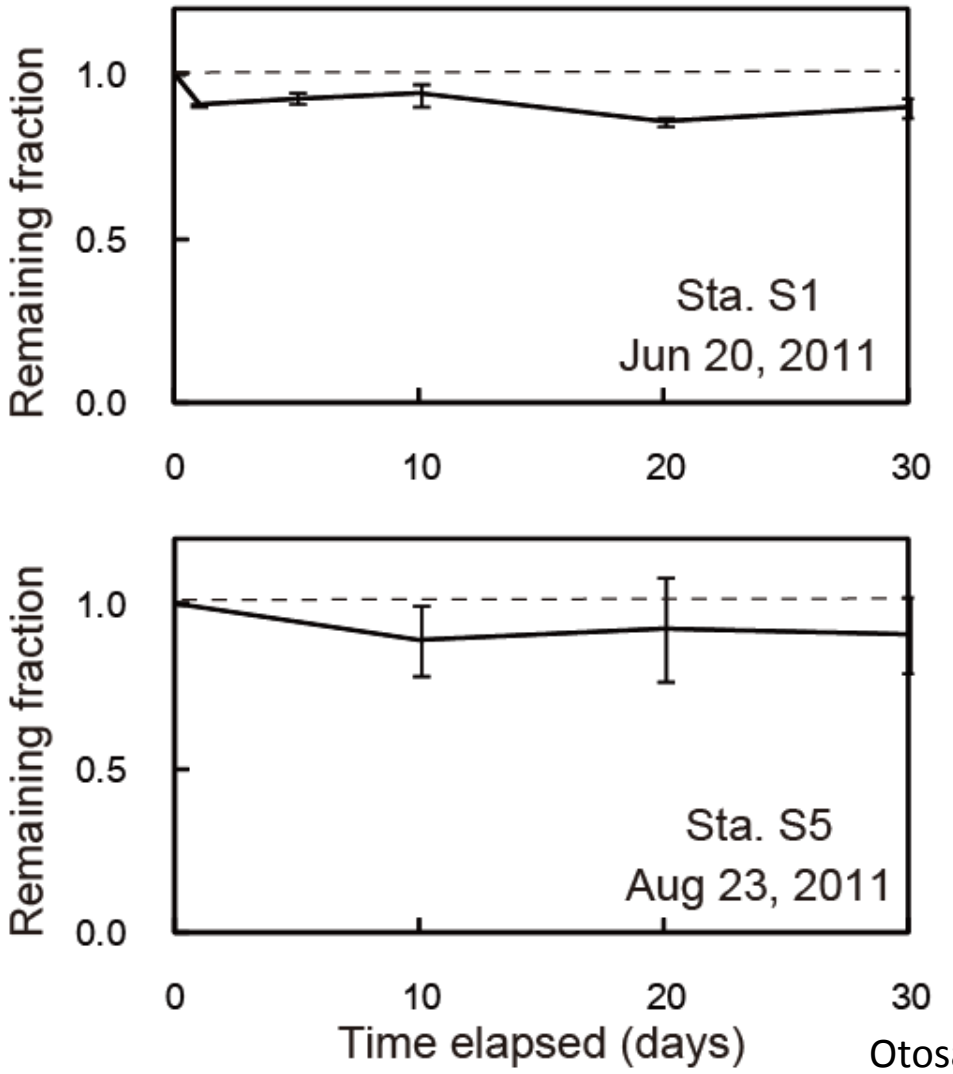

Otosaka and Kobayashi, Fig 5

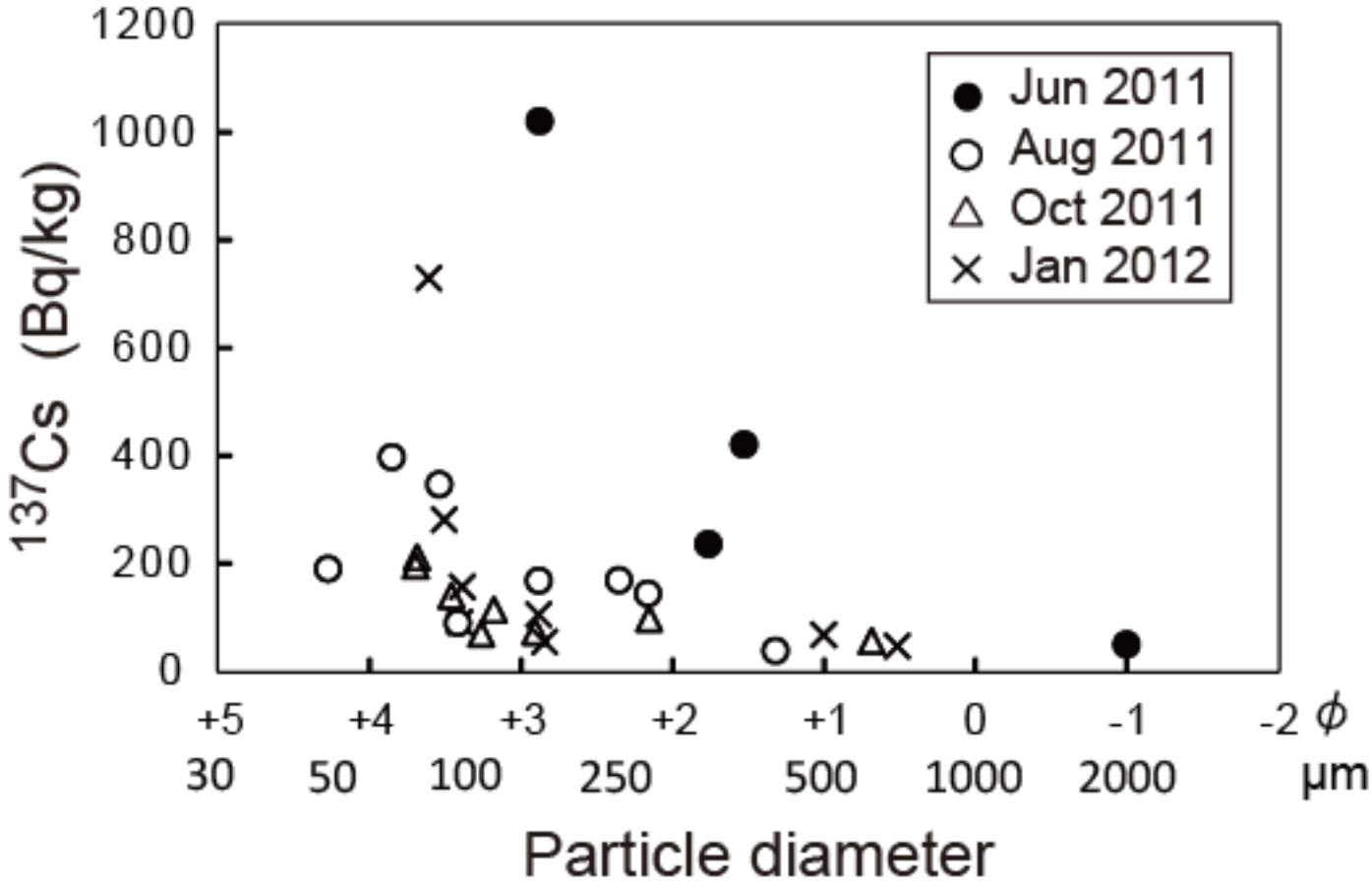

Otosaka and Kobayashi, Fig 6

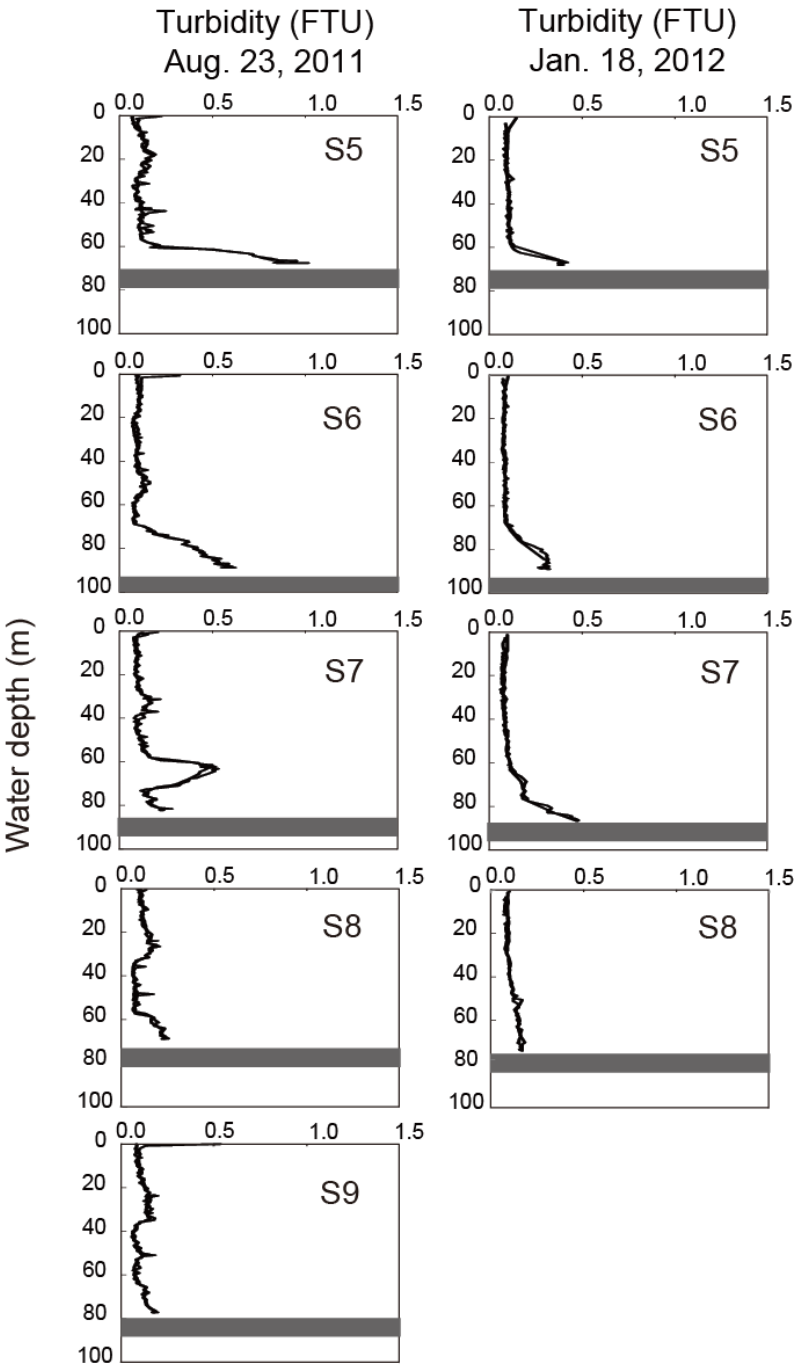

Otosaka and Kobayashi, Fig 7